Investigating the Environment of the Indiana and Ohio Tornado Outbreak of 24 August 2016 Using a WRF Model Simulation

Kevin Gray and Jeffrey Frame

Department of Atmospheric Sciences, University of Illinois at Urbana-Champaign, Urbana, IL

1. Introduction

On 24 August 2016, a tornado outbreak impacted Indiana and Ohio with 22 confirmed tornadoes. These tornadoes occurred well outside of the 2% risk area outlined in the 1300 UTC Storm Prediction Center Convective Outlook (Fig. 1). Forecasting the outbreak proved challenging since many morning convection-allowing models did not depict cellular convection or significant updraft helicity across this area. Nevertheless, strong low-level shear, adequate deep-layer shear, low lifting condensation levels, and plentiful instability provided an environment favorable for the development of supercells and tornadoes. Of particular interest is the transition of convection from disorganized linear convection to supercellular convection between 1700 and 1900 UTC, after which time tornadoes began to occur. This transition occurred soon after the storms became surface based.

The purpose of this study is to understand how the convection evolved as it organized into surface-based supercells and how environmental factors may have facilitated this transition. The study is carried out via the analysis of environmental parameters, radar observations, and a high-resolution Weather Research and Forecasting (WRF) model simulation.

The mesoscale environment during the event is presented in section 2. Radar observations are described in section 3 and output from the WRF simulation is presented in section 4. Lastly, conclusions and future work are discussed in section 5.

2. Mesoscale environment

An 1800 UTC Rapid Refresh Model (RAP) analysis depicts a mesoscale convective vortex (MCV) over northern Illinois. On the southern flank of this MCV, the 500 mb flow exceeded 40 kts over central Illinois and Indiana (Fig. 2a). At 700 mb, slight warm air advection occurred between 1200 and 1800 UTC, bringing temperatures at this level to 8-10°C across Indiana, resulting in only a weak cap (Fig. 2b). At 925 mb, winds were on the order of 30 knots over this same area, yielding strong low-level vertical wind shear (Fig. 2c). At the surface, a wind shift from southerly to gusty southwesterly flow (purple line in Fig. 2d) moved northeastward amidst a moist air mass characterized by dewpoints of 71-74°F.

The 1200 UTC sounding from Lincoln, IL (star in Fig. 2a), depicts nearly 30 kts of vertical wind shear in the surface to 925 mb layer, with little shear above this layer. This means that surface-based storms had access to strong wind shear in the lowest km, while elevated storms, feeding from air above 925 mb, would only be weakly sheared and thus disorganized (Fig. 2e). At this time, there was 66 J kg^{-1} of mixed-layer CIN, prohibiting surface-based storm formation, but parcels lifted from near 800 mb were relatively uninhibited.

By 1800 UTC, mixed-layer CIN over central Indiana was negligible in the presence of 2000-3000 J kg^{-1} CAPE (Fig. 2f). Additionally the 0-1 km storm-relative helicity (SRH) was well above 100 m^2 s^{-2} over Indiana, more than sufficient for the development of rotating storms (Davies-Jones et al. 1990; Thompson et al. 2012; Fig. 2g).

3. Radar analysis

a. Mesoscale overview

On the morning of 24 August, disorganized elevated convection moved from Illinois into Indiana between 1200 and 1500 UTC. This first round of convection eventually dissipated over Indiana (not shown).

Later, between 1500 and 1700 UTC, a second round of elevated convection developed over eastern Illinois (Fig. 3a). This convection was loosely organized into a line oriented from southwest to northeast. A surging outflow boundary was not observed on radar as this convection moved into Indiana around 1800 UTC (Fig. 3a). While radar data below 1500 m were limited owing to the location of the convection between the Lincoln, IL (KILX), and Indianapolis, IN (KIND), radars, surface observations similarly depict a lack of strong outflow with these storms (Fig. 2d).

The first supercell began to organize on the southern edge of this convection, near Crawfordsville, IN, between 1800 and 1900 UTC (Fig. 3b), producing an EF-1 tornado near Crawfordsville at 1838 UTC. Shortly after the Crawfordsville supercell developed, another supercell formed to its north near Kokomo, IN (Fig. 3b). This supercell produced an EF-3 tornado as it approached Kokomo at 1920 UTC. The Crawfordsville cell underwent cell mergers as it moved eastward toward Indianapolis while the Kokomo storm cycled and also moved eastward toward Marion (Fig. 3c).

A third supercell formed near Fort Wayne, IN, around 2100 UTC (Fig. 3d). This storm also produced an EF-3 tornado in Woodburn, IN, just east of Fort Wayne near the Ohio border, and at least four other tornadoes in northwestern Ohio. To the west of these three supercells, several other small supercells formed between 2000 and 2100 UTC (Fig. 3d), some of which also produced tornadoes.

b. Storm-scale analysis

The storm that became the Crawfordsville supercell was initially multicellular, with new cells forming to its south and older, decaying cells to its north (Fig. 4a). Weak rotation developed within the most dominant of these cells around 1300 m above ground level (AGL; see white circle in Fig. 4b) at 1758 UTC. This storm began to exhibit supercellular structure by 1821 UTC with the formation of a sharp reflectivity gradient on its southern flank and a slight echo appendage on its southwestern side (Fig. 4c). At this time, rotation within the storm weakened and shifted rearward, while low-level convergence strengthened ahead of the storm in the inflow region (Fig. 4d). As a small cell south of the developing supercell approached it (Fig. 4e), the convergence and rotation associated with the developing supercell increased significantly, possibly owing to the formation of a rear-flank downdraft (Fig. 4f). As convergence continued to increase, the vertical vorticity was likely amplified via stretching, and the storm produced a tornado between 1838-1848 UTC.

4. WRF model simulation

a. Model configuration

The WRF Model (version 3.8.1; Skamarock et al. 2008) was used to simulate this event. The model was initialized from the 0600 UTC 24 August 2016 NAM analysis. Three nested grids were utilized with horizontal resolutions of 12 km, 4 km, and 1 km (Fig. 5); 60 vertical levels were used on all grids. We used the Morrison 2-moment microphysics package (Morrison and Grabowski 2007) and the YSU boundary layer parameterization (Hong et al. 2006). The Kain-Fritsch convective parameterization was used on the 12 km domain only (Kain 2003).

b. Simulated environment – 1700 UTC

The simulation captures the MCV at 500 mb over northern Illinois, with winds on the order of 40 kts on its southern flank as in the RAP analysis (Figs. 2a and 6a). Across most of Indiana, 0-1 km SRH is greater than 100 $m^2 s^{-2}$, with mixed-layer CAPE over 2000 J kg^{-1}, also as in the RAP analysis. (Figs. 2f, 2g, 6b, and 6c). Model soundings (generated at the red star in Fig. 6c) reveal that surface-based CIN is removed in the near-storm environment between 1630 and 1725 UTC (Figs. 6d and 6e). The remaining analysis herein focuses on output on the 1 km grid.

c. Mesoscale evolution of simulated convection

In the simulation, quasi-linear convection crosses from Illinois into Indiana at 1630 UTC (Fig. 7a), slightly earlier than was observed (Fig. 3a). A dominant supercell develops and persists on the southwestern end of the line, consistent with observations (Figs. 3b, 7b, and 7c). Although transient rotation develops farther northeast within the line (Figs. 7c and 7d), the model fails to develop additional supercells from this initial convection in northeastern Indiana. It is possible that too much stratiform precipitation ahead of the linear convection (Figs. 7a and 7b), or too much outflow (compare Figs. 2f and 6c) may have limited instability farther north, thus preventing the development of additional supercells in northeastern Indiana. The simulated storms are oriented more east-west than was observed (Figs. 3b and 7c).

d. Storm-scale analysis

On its southern end, the simulated convection is quasi-linear with only weak outflow as indicated by the wind field and temperature deficits around 3°C at 1700 UTC. At this time, any vertical relative vorticity (ζ) at 1 km associated with the storms is generated by horizontal shear across the gust front (Fig. 8a). Small cells form south of and merge with the southwestern end of the stronger convection, similar to the radar observations. A localized area of convergence develops at the far southwestern end of the stronger convection, focusing ζ in this region (Fig. 8b). At 1725 UTC, when the model sounding indicates an uncapped inflow environment, an inflow notch forms and ζ becomes concentrated near the inflow notch (Fig. 8c). By 1745 UTC, the storm is a mature supercell with $\zeta > 0.015\ s^{-1}$ at 1 km, a hook echo, and forward-flank and rear-flank gust fronts as indicated by the temperature and wind fields (Fig. 8d).

5. Conclusions and future work

On 24 August 2016, a surprise tornado outbreak impacted parts of Indiana and Ohio. The convection transitioned from disorganized elevated convection to discrete tornadic supercells just after it became surface based and gained access to strong near-surface vertical wind shear. The event proved difficult to forecast for many operational convection-allowing models.

A WRF model simulation of this event captures the thermodynamic and kinematic environment, including the MCV, which regionally augmented the vertical wind shear. As in the observations, robust supercellular convection did not develop in the simulation until the storms became surface based. The lack of strong outflow in both the observed and simulated storms likely aided in this transition to a supercellular mode.

Future work includes exploring additional cloud microphysics options in the WRF simulation and performing additional analysis of the transition from elevated to surface-based convection. We also plan to examine why many operational models failed to develop supercellular convection in this regime.

Acknowledgments. We are grateful to Professor Steve Nesbitt of the University Of Illinois at Urbana-Champaign for assistance with the WRF model and Zachary Hargrove of the National Weather Service Forecast Office at Bismarck, ND, for sharing plotting routines for the WRF output.

REFERENCES

Davies-Jones, R. P., D. W. Burgess, and M. Foster, 1990: Test of helicity as a tornado forecast parameter. *Preprints, 16th Conf. on Severe Local Storms*, Kananaskis Park, AB, Canada, Amer. Meteor. Soc., 588-592.

Hong, S.-Y., Y. Noh, and J. Dudhia, 2006: A new vertical diffusion package with an explicit treatment of entrainment processes. *Mon. Wea. Rev.*, **134**, 2318-2341.

Kain, J. S., 2003: The Kain-Fritsch Convective Parameterization: An Update. *Journal of Applied Meteorology*, **43**, 170-181.

Morrison, H., and W. W. Grabowski, 2007: A Novel Approach for Representing Ice Microphysics in Models: Description and Tests Using a Kinematic Framework. *Journal of the Atmospheric Sciences*, **65**, 1528-1548.

Skamarock, W. C., and Coauthors, 2008: *A Description of the Advanced Research WRF Version 3*. NCAR Technical Note NCAR/TN-475+STR, doi:10.5065/D68S4MVH.

Thompson, R. L., B. T. Smith, J. S. Grams, A. R. Dean, C. Broyles, 2012: Convective Modes for Significant Severe Thunderstorms in the Contiguous United States. Part II: Supercell and QLCS Tornado Environments. *Wea. Forecasting*, **27**, 1136-1154.

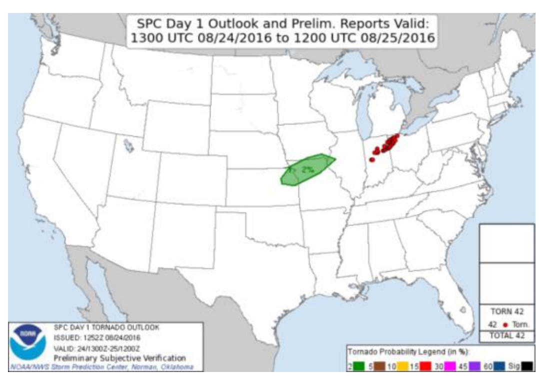

Figure 1: Storm Prediction Center (SPC) 1300 UTC 24 August 2016 tornado outlook (green shading) and preliminary tornado reports (red dots).

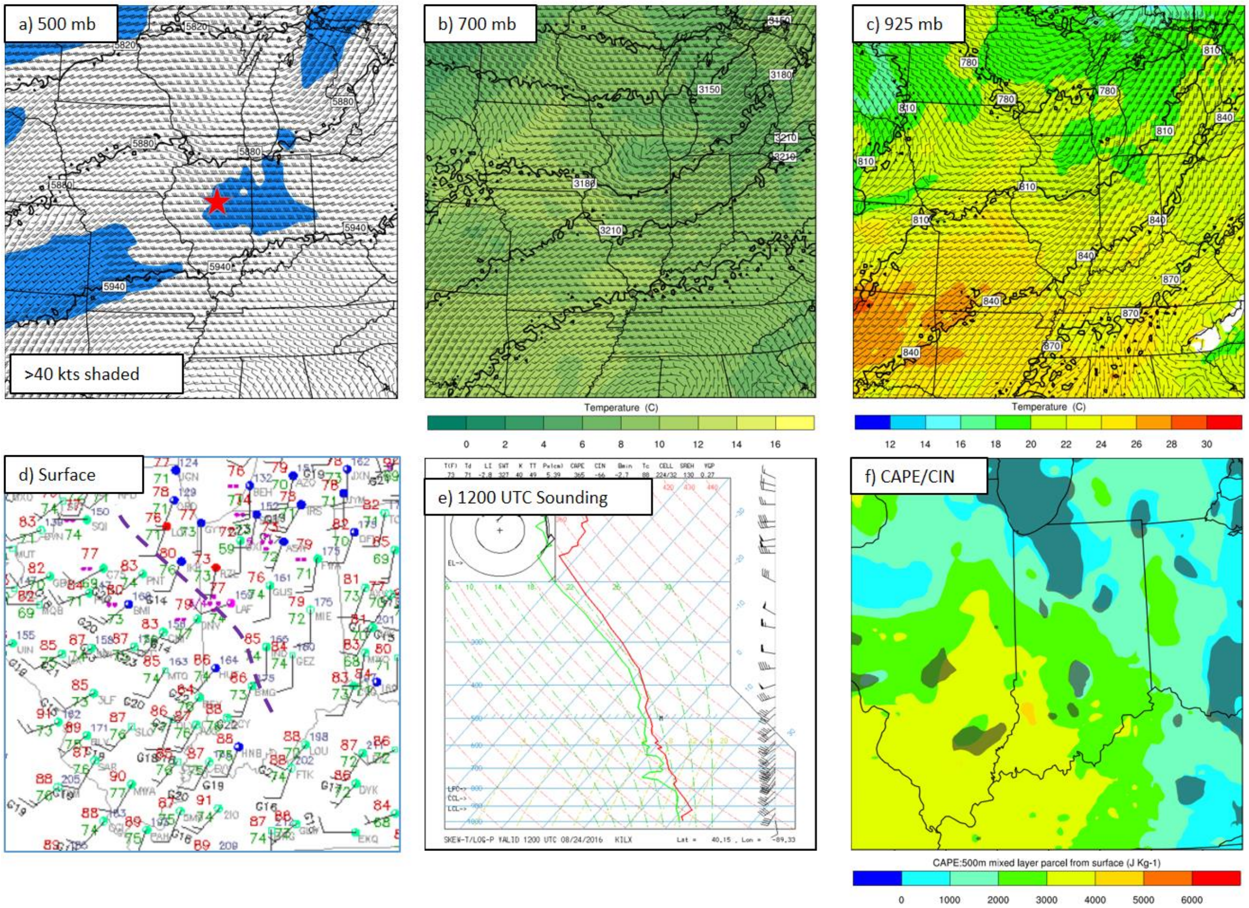

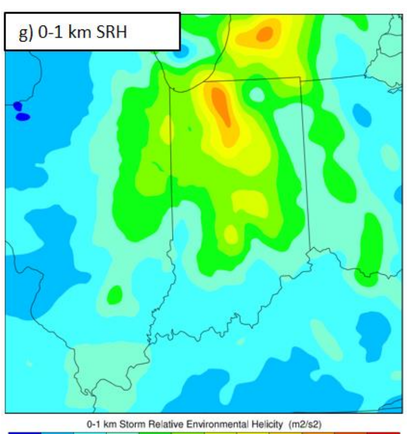

Figure 2: RAP analyses valid at 1800 UTC 24 August 2016: (a) 500 mb height (m) and wind (kts; > 40 kts shaded); (b) 700 mb height (m), wind (kts), and temperature (°C); (c) 925 mb height (m), wind (kts), temperature (°C); (d) surface observations (°F, kts); (e) 1200 UTC sounding from Lincoln, IL; (f) 500 m mixed-layer CAPE and CIN (> 10 J kg^{-1} CIN shaded gray); and (g) 0-1 km SRH (m^2 s^{-2}).

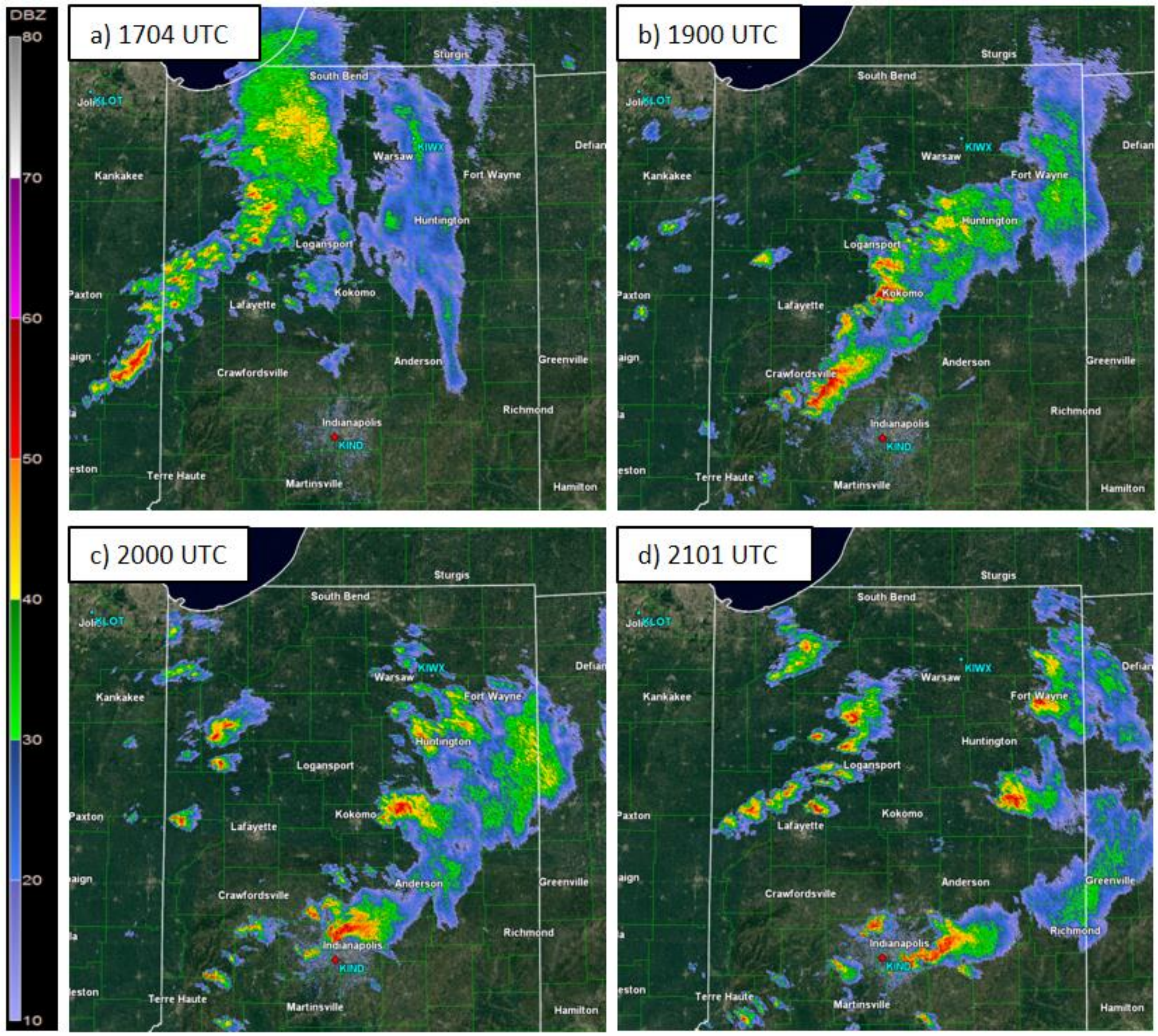

Figure 3: Indianapolis, IN (KIND), WSR-88D radar reflectivity at (a) 1704, (b) 1900, (c) 2000, and (d) 2101 UTC. The red dot in the south-central portion of the images indicates the radar location.

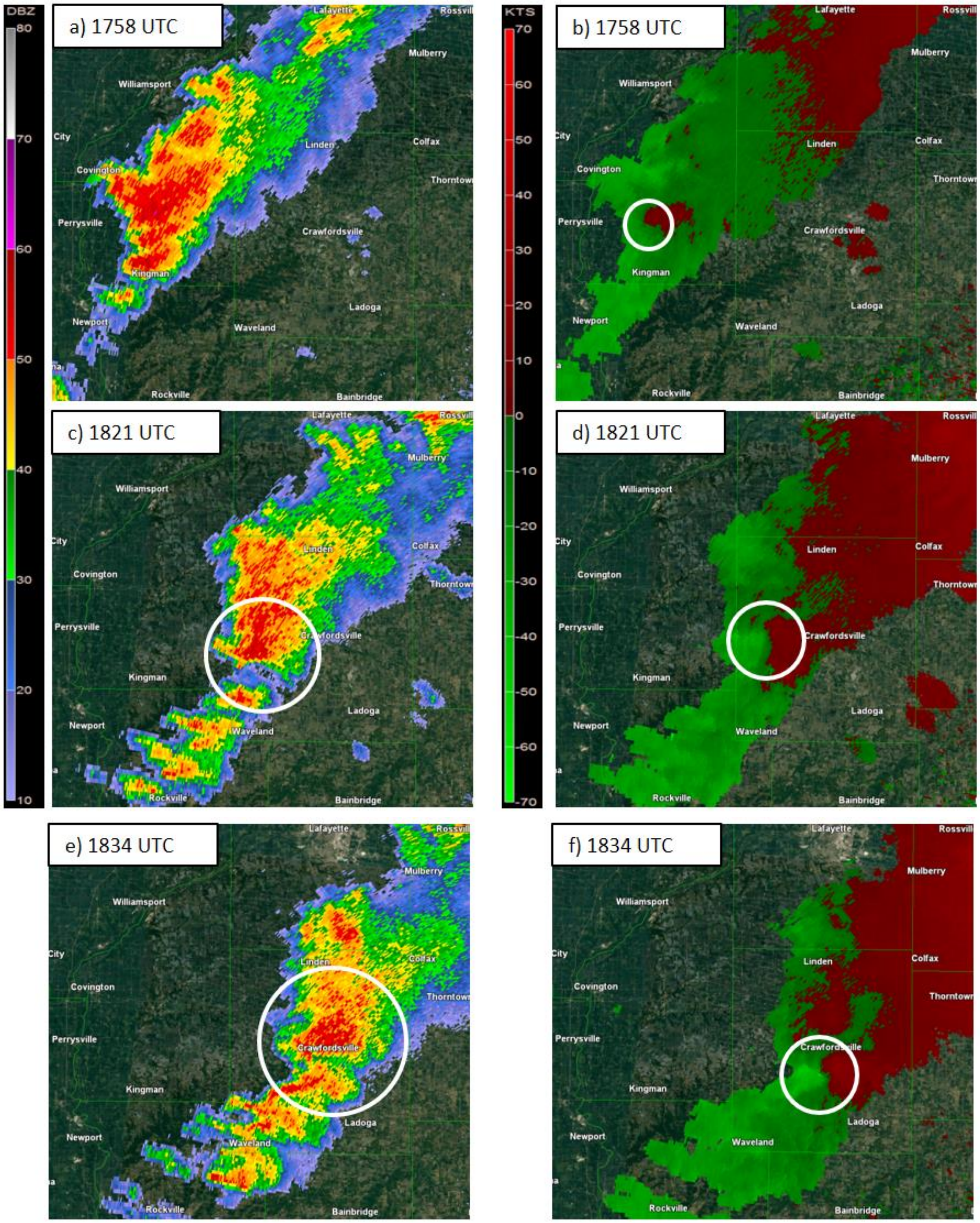

Figure 4: Indianapolis, IN (KIND), WSR-88D (a) radar reflectivity (dBZ) at 1758 UTC, (b) radial velocity (m s^{-1}) at 1758 UTC, (c) radar reflectivity at 1821 UTC, (d) radial velocity at 1821 UTC, (e) radar reflectivity at 1834 UTC, (f) radial velocity at 1834 UTC. Radar location is to the southeast of the storm.

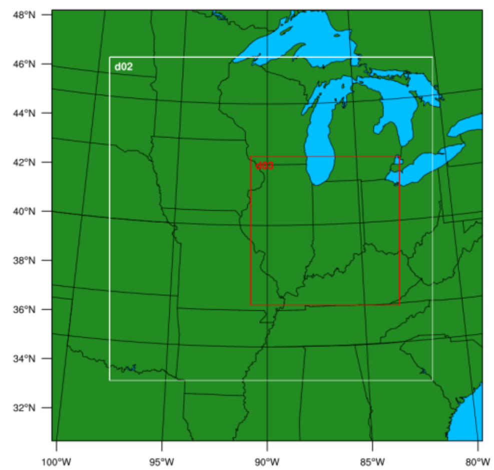

Figure 5: Map of the three nested WRF domains with horizontal resolutions of 12 km, 4 km, and 1 km.

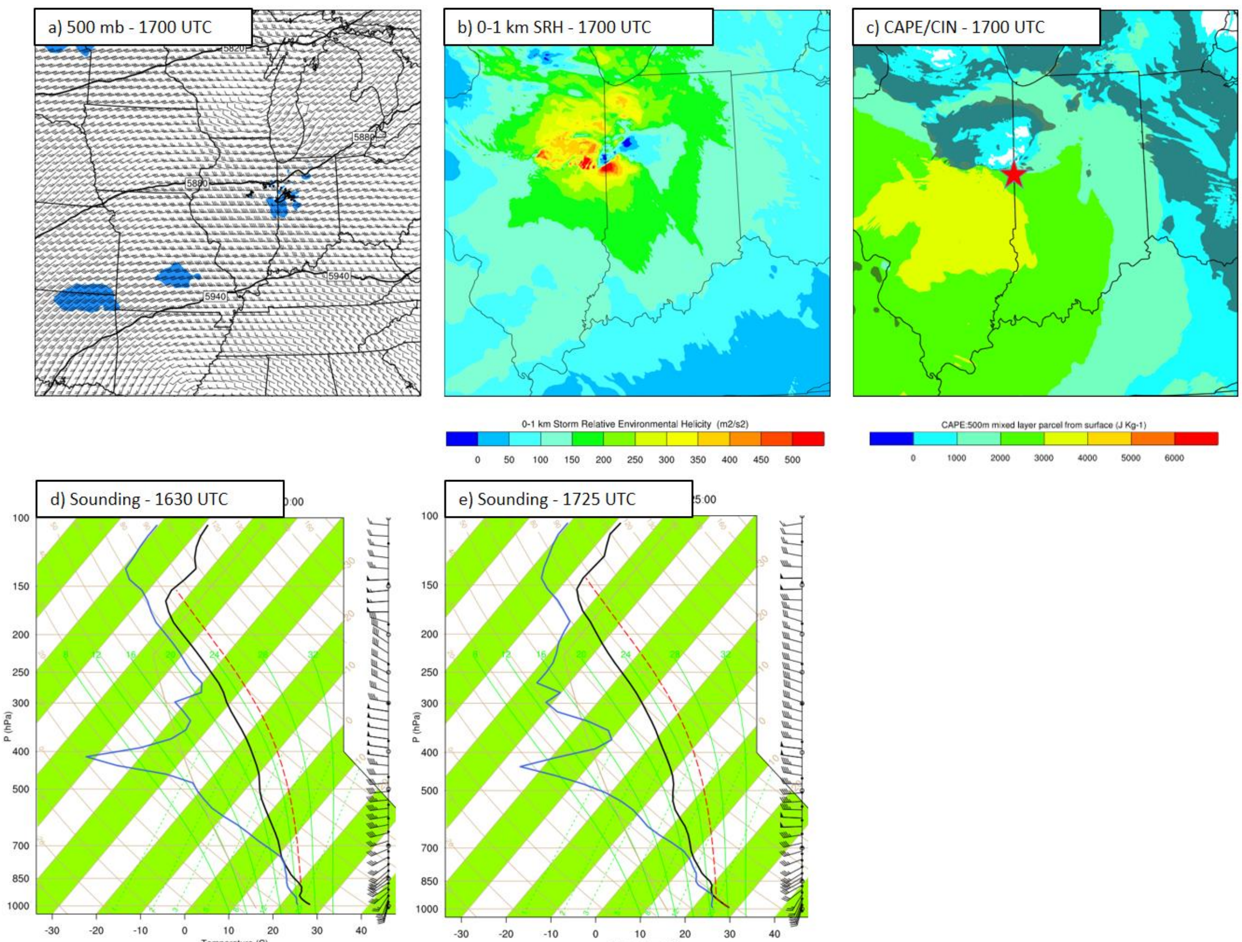

Figure 6: WRF model simulated (a) 500 mb height (m) and wind (kts; > 40 kts shaded) at 1700 UTC on 4 km grid; (b) 0-1 km SRH (m^2 s^{-2}) at 1700 UTC on 1 km grid; (c) 500 m mixed-layer CAPE and CIN (> 10 J kg^{-1} CIN shaded gray) at 1700 UTC on 1 km grid; model soundings at the red star in (c) at (d) 1630 and (e) 1725 UTC.

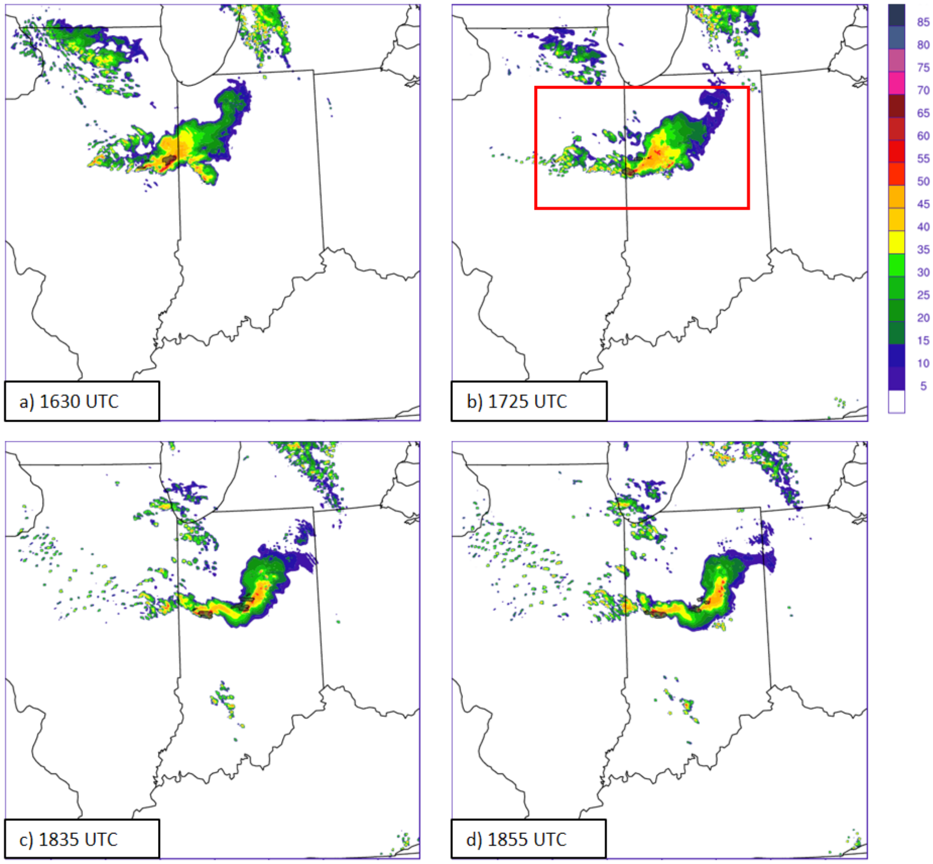

Figure 7: Simulated 1 km radar reflectivity and updraft helicity greater than 300 m^2 s^{-2} over the 30 minutes prior to each image (dark shading) at (a) 1630, (b) 1725, (c) 1835, and (d) 1855 UTC. Red box indicates region depicted in Fig. 8.

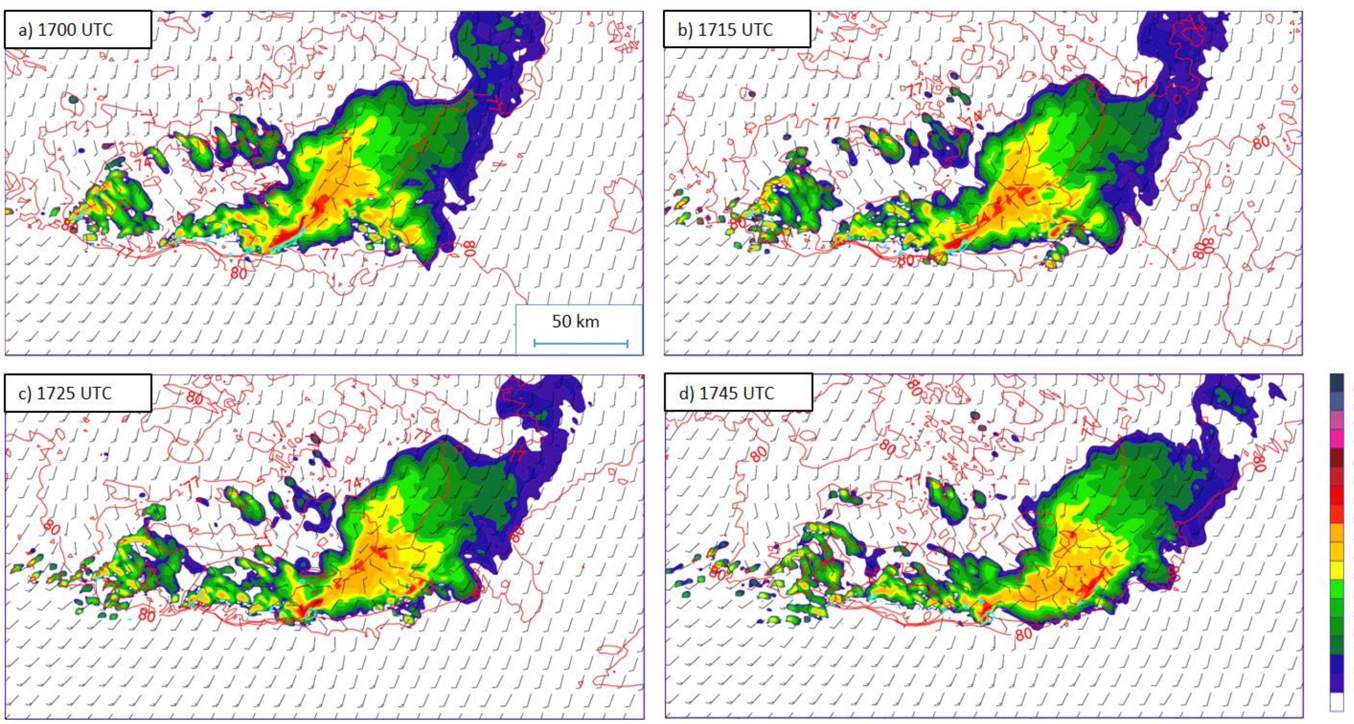

Figure 8: Simulated 1 km radar reflectivity (shaded), 10 m winds (barbs; kts),1 km vertical vorticity contoured only at 0.005 s^{-1} (cyan), and isotherms contoured between 74-80°F every 3°F (red) at (a) 1700, (b) 1715, (c) 1725, and (d) 1745 UTC in the boxed region in Fig. 7b. State borders removed for clarity.